Opportunistic Spectrum Access for Mobile Cognitive Radios

Alexander W. Min,[†‡] Kyu-Han Kim,[§] Jatinder Pal Singh,[§] and Kang G. Shin[†]
[†]Real-Time Computing Laboratory, Dept. of EECS, The University of Michigan, Ann Arbor, MI 48109
[§]Deutsche Telekom Inc. R&D Lab USA, Los Altos, CA 94022
{alexmin, kgshin}@eecs.umich.edu, {kyu-han.kim, jatinder.singh}@telekom.com

***Abstract*—Cognitive radios (CRs) can mitigate the impending spectrum scarcity problem by utilizing their capability of accessing licensed spectrum bands opportunistically. While most existing work focuses on enabling such opportunistic spectrum access for *stationary* CRs, mobility is an important concern to secondary users (SUs) because future mobile devices are expected to incorporate CR functionality. In this paper, we identify and address three fundamental challenges encountered specifically by *mobile* SUs. First, we model channel availability experienced by a mobile SU as a two-state continuous-time Markov chain (CTMC) and verify its accuracy via in-depth simulation. Then, to protect primary/incumbent communications from SU interference, we introduce *guard distance* in the space domain and derive the optimal guard distance that maximizes the spatio-temporal spectrum opportunities available to mobile CRs. To facilitate efficient spectrum sharing, we formulate the problem of maximizing secondary network throughput within a convex optimization framework, and derive an optimal, distributed channel selection strategy. Our simulation results show that the proposed spectrum sensing and distributed channel access schemes improve network throughput and fairness significantly, and reduce SU energy consumption for spectrum sensing by up to** $74\,\%$**.**

I. Introduction

The recent advent of cognitive radio (CR) technology promises significant improvement in spectrum efficiency by allowing secondary (unlicensed) devices or users (SUs) to opportunistically utilize the licensed spectrum bands. Such opportunistic spectrum access has attracted considerable interest due to its ability to alleviate the spectrum scarcity problem that we may face soon because of the rapid increase in wireless spectrum demand and the inefficiency of current static spectrum allocation policies.

The main goal of opportunistic spectrum access is to allow CR-equipped SUs to safely coexist with legacy primary devices or users (PUs) without disrupting PU communications. To achieve this goal, various aspects of opportunistic spectrum access, such as spectrum sensing [1]–[3], spectrum sharing [4], [5], and security [6], have been studied extensively. Most existing efforts, however, focus on stationary cognitive radio networks (CRNs), in which both PUs and SUs are stationary, and thus, they may not be suitable when SUs are *mobile*. We envision that future mobile devices will incorporate CR-functionality and will be capable of dynamic and flexible spectrum access. Meanwhile, various standardization efforts for mobile CRs are being developed to utilize spectrum white spaces, such as 802.11af [7] and Ecma 392 [8]. Enabling opportunistic spectrum access for mobile SUs, however, entails new practical challenges, and remains an open problem.

‡ Alexander W. Min was a Research Intern at Deutsche Telekom Inc. R&D Labs USA while this work was conducted.

In this paper, we study the problem of enabling opportunistic spectrum access for *mobile* CR devices by identifying and addressing three fundamental challenges. First, existing spectrum-availability models are derived based solely on PUs' temporal traffic statistics and might thus be unsuitable for CRNs with mobile CRs/SUs. Unlike in stationary CRNs (e.g., [9]), in which the spectrum opportunity (or availability) is mostly affected by PUs' temporal channel usage patterns, in mobile CRNs, availability can also change as SUs move towards or away from PUs that are actively transmitting data. To overcome this limitation, we model channel availability—that reflects the fluctuation of spectrum opportunities induced by the SU mobility—as a two-state continuous-time Markov chain (CTMC) and verify its accuracy via in-depth simulation.

Second, protecting PUs from the SU mobility-induced interference is a challenging problem that calls for an efficient spectrum-sensing strategy tailored to mobile CRNs. Mobile SUs may need to sense spectrum more frequently to avoid interfering with PU communications. However, frequent spectrum sensing may not only incur significant time overhead [1], but also quickly drain the battery of mobile CR devices due to the power-intensive nature of spectrum sensing [10], [11]. To address this challenge, we propose the use of *guard distance* to minimize the required spectrum sensing for mobile SUs, while providing sufficient protection to primary communications. Guard distance is an additional separation between PUs and SUs to prevent mobile SUs from causing excessive interference. Further, based on our proposed channel-availability model, we jointly optimize the guard distance and spectrum-sensing interval to maximize the reuse of spectrum opportunities in the space and time domains.

Third, mobile SUs will experience heterogeneous spectrum opportunities across the space and time domains based on the geographical distribution of PUs and SUs' mobility patterns. To better utilize such heterogeneous spectrum opportunities, we derive an optimal, distributed channel-access strategy in a closed form within the convex optimization framework. Our channel-access strategy incorporates the three key factors that diversify spectrum access opportunities across different channels: (i) SU-mobility-aware spectrum sensing adaptation, (ii) heterogeneity in PUs' spatial distributions and channel-usage patterns, and (iii) spectrum sharing among SUs. Our proposed channel-access strategy is shown to significantly improve the secondary network throughput, fairness and energy-efficiency in spectrum sensing.

The three challenges mentioned above are inter-related. Hence, to fully realize the benefits of opportunistic spectrum access for mobile SUs, they must be considered jointly. To the best of our knowledge, our work is the first to extensively investigate SU mobility in regard to the channel-availability model, spectrum sensing and access strategies.

The remainder of this paper is organized as follows. Section II overviews related work, and Section III introduces the system models that will be used throughout the paper. Section IV presents our new channel-availability model for mobile SUs. Sections V and VI detail the design of spectrum sensing and access schemes that maximize the secondary network throughput. Section VII evaluates the performance of the proposed schemes, and Section VIII concludes the paper.

II. Related Work

Spectrum sensing has been studied extensively as a key technology for primary detection and protection [1], [2], [12]–[16]. Most existing work, however, focuses on optimizing the sensing interval based on PUs' *temporal* channel-usage statistics. To validate such channel models, Wellens *et al.* [16] studied the impact of channel-occupancy statistics obtained from extensive measurements on the performance of MAC-layer sensing schemes. They showed that the channels with longer `busy`/`idle` periods follow exponential distributions and that spectrum sensing and access strategies designed under the assumption of exponentially-distributed PU traffic are highly efficient. However, such models hinge on the assumption of *stationary* CRNs, in which both PUs and SUs are stationary. Thus, they may not be suitable for *mobile* CRNs, in which channel availability depends on dynamically changing SUs' locations. By contrast, we model channel availability from a mobile SU's perspective by incorporating the impact of SU mobility (e.g., speed).

Despite its practical importance, the problem of allowing mobile SUs in CRNs has received little attention. The IEEE 802.22 standard draft provides a two-stage sensing (TSS) mechanism [17], but it is designed exclusively for the detection of a stationary TV transmitter, and does not specify any efficient mechanisms for spectrum sensing for portable/mobile CRs. Recently, the FCC [18] imposed a minimum sensing interval of 60 seconds for TV band devices (TVBD). However, this may not be sufficient to protect PUs from the interference induced by SU mobility. Moreover, while most previous work focused on either scheduling spectrum sensing [2] or spatial CR deployment [19], [20] for primary protection, we *jointly* exploit the guard distance and the sensing interval to maximize spatio-temporal spectrum opportunities for mobile SUs.

III. System Model

In this section, we present a mobile CRN model, along with distributed spectrum sensing and channel-access models.

A. Mobile CRN Model

We consider a CRN with infrastructure-based *fixed* primary networks and *mobile* ad-hoc secondary networks in the same geographical area, as shown in Fig. 1. We assume that each cell of the primary system consists of a single central node (e.g., access point) and receivers. From now on, we refer to each primary cell as a PU. We assume that there is a non-empty set $\mathcal{K}$ of licensed channels, and that PUs operating on the same channel belong to the same type of system and have the same *temporal* channel-usage statistics, e.g., channel `busy`/`idle` durations.[1] Primary transmitters are assumed to be distributed, following a point Poisson process with a different average density for each channel, i.e., $n_{p,i} \sim Poisson(k; \rho_{p,i})$, where $n_{p,i}$ is the number of primary transmitters and $\rho_{p,i}$ is the average PU density on channel $i \in \mathcal{K}$. We assume that primary transmitters on the licensed channel $i \in \mathcal{K}$ are separated by at least twice their transmission range in order to avoid interference [21]. Such a PU distribution can be obtained by eliminating overlapping PUs in the original Poisson process, resulting in a *Marten Hardcore Process* [22]. We assume that SUs know the average density of PUs on each channel, and PUs' temporal channel-usage characteristics. We further assume that SUs do not know the availability of a channel at specific time and location unless they perform spectrum sensing.

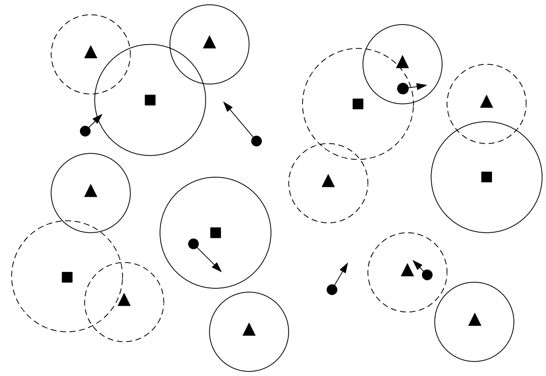

Fig. 1. **Illustration of a mobile CRN:** Mobile CR devices (solid dots with arrow) can opportunistically use the licensed channels only when the distance from any active PUs (triangles and rectangles) is greater than a certain threshold (i.e., protection region) so as to avoid excessive interference to PUs. The circles with solid (dotted) lines indicate the protection region of active (inactive) PUs with (without) data transmission.

B. Distributed Spectrum Sensing & Access Models

We assume that SUs are *mobile* devices with CR-functionality that allows them to access any licensed channels in the set $\mathcal{K}$. However, they do not have the capability of accessing a geo-location spectrum database to obtain local spectrum-availability information.[2] Therefore, we assume that SUs rely on local spectrum sensing (e.g., feature detection) to detect channel availability—i.e., the presence/absence of primary signals—at a given time and location. SUs are assumed to use feature detection (e.g., [23]) for PHY-layer sensing. Feature detection is known to provide high accuracy without collaboration amongst SUs even at a low SNR [24]. Thus, it is better suited for ad-hoc secondary networks, in which SU collaboration may not be feasible due to the needs for information exchange and global time synchronization [25].

Once an SU identifies available channels via spectrum sensing, it contends with neighboring SUs to access the channel via a random access scheme such as CSMA. SU channel access behavior is depicted in Fig. 2. We assume that SUs

[1] We use the terms `busy`/`idle` to indicate PUs' temporal traffic patterns, and use ON/OFF to indicate the availability of a channel seen from a mobile SU's perspective.

[2] The FCC specifies two types (Mode I and II) of portable devices that can access TV white space [18]. Mode I devices are required to access the geo-location database, whereas Mode II devices are not required such access capability.

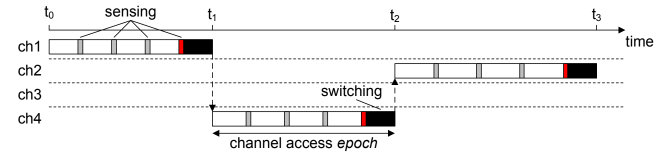

Fig. 2. **Opportunistic channel access model:** An SU periodically senses its current operating (in-band) channel (the gray block) until it detects a primary signal, followed by channel switching (the black block). The sensing interval is dynamically adapted based on the SU's speed and PUs' spatio-temporal channel usage statistics.

always have packets to transmit and always use the maximum transmission power allowed by a regulatory body.

IV. Modeling Channel Availability for Mobile Secondary Users

In this section, we characterize the spectrum opportunity that corresponds to PUs' spatio-temporal channel usage patterns, propose a new SU mobility-aware channel availability model, and demonstrate its accuracy via simulation.

A. Characterizing Spatio-Temporal Spectrum Opportunity

We first introduce the keep-out-radius and guard distance for protecting PUs from increased interference caused by SU mobility. We then quantify the spatio-temporal spectrum opportunities available to mobile SUs.

Definition 1 *(Keep-out radius) The keep-out radius is defined as the minimum distance between a primary transmitter and SUs under the* interference temperature limit *(*`ITL`*) set by the regulatory body (e.g., the FCC), i.e.,*

$$R_{e,i} = \inf\left\{ d \in \mathbb{R} \,\middle|\, I_{tot}(\rho_{s,i}, d) \le \texttt{ITL} \right\}, \tag{1}$$

where $I_{tot}(\rho_{s,i}, d)$ is the average interference generated by SUs (separated by least distance d from the primary transmitter) at a primary receiver located at the edge of the primary coverage area and $\rho_{s,i}$ is the density of SUs on channel i.

The aggregate SU interference at a primary receiver located at the edge of the primary transmission range (i.e., at distance R_o from the primary transmitter) can be bounded as [19]:

$$I_i^U(\rho_{s,i}, R_{e,i}) = \frac{2\pi P_o d_o^\alpha \rho_{s,i}}{\alpha - 2} \left(R_{e,i} - R_o\right)^{2-\alpha}, \tag{2}$$

where P_o is the transmission power of SUs, d_o the short reference distance (e.g., $5\,\mathrm{m}$), α the path-loss exponent, $\rho_{s,i}$ the average SU density on channel i, R_o the PUs' transmission range, and $R_{e,i}$ the primary keep-out radius.

From Eq. (2), the keep-out radius necessary for channel i to meet the interference constraint, $I_i^U \le \texttt{ITL}$, is given as:

$$R_{e,i}^*(\rho_{s,i}) = \left[\left(\frac{(\alpha - 2)}{2\pi P_o d_o^\alpha \rho_{s,i}} \cdot \texttt{ITL} \right)^{\frac{1}{2-\alpha}} \right]^+ + R_o, \tag{3}$$

where $[\bullet]^+ \triangleq \max\{\bullet, 0\}$.

One important observation from Eq. (3) is that the keep-out radius of channel i increases with the density of channel-i SUs, $\rho_{s,i}$, as shown in Fig. 3(a). This is because as SU density increases (i.e., more SUs access channel i), the keep-out radius must be expanded to meet the interference constraint.

The keep-out radius in Eq. (3), however, assumes *stationary* SUs, and thus, it may not be sufficient to protect PUs from interference caused by mobile SUs. To protect PUs further

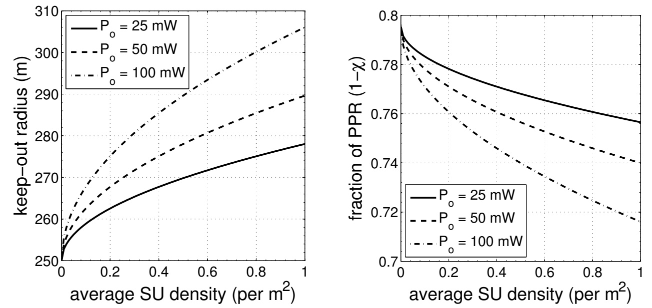

(a) Keep-out radius (b) Fraction of available area

Fig. 3. **Impact of SU density on spatial spectrum opportunity:** The keep-out radius for primary protection (a) increases with increasing SU density, and thus (b) spatial spectrum opportunity decreases. The simulation parameters are set to $R_o = 250\,\mathrm{m}$, $\texttt{ITL} = 0.1\,\mathrm{mW}$, $\rho_p = 1/\mathrm{km}^2$, and $\alpha = 4$.

from such SU mobility-induced interference, we introduce an additional protection layer (*guard distance*), denoted by ϵ_i.

Definition 2 *(Primary protection region) Let $\mathcal{P}_i$ denote a set of primary transmitters on channel i. A* primary protection region *(PPR) of primary transmitter $j \in \mathcal{P}_i$, denoted as $\Omega_{i,j}$, is defined as a unit disk centered at the primary transmitter j located at $(x_{i,j}, y_{i,j})$, i.e.,*

$$\Omega_{i,j} = \left\{ (x, y) \in \mathbb{R}^2 \,\middle|\, \|(x_{i,j}, y_{i,j}) - (x, y)\| \le R_{e,i} + \epsilon_i \right\}, \tag{4}$$

where $R_{e,i}$ is the keep-out radius*, and ϵ_i is the guard distance.*

Thus, if an SU is located within a PPR of active PUs on channel i, it refrains from using the same channel to avoid causing interference.

Then, the average fraction of the union of PPRs on channel i in the entire network is [26]:

$$\chi_i(\rho_{s,i}) = 1 - e^{-\rho_{p,i}\pi(R_{e,i}(\rho_{s,i}) + \epsilon_i)^2}, \tag{5}$$

where $\rho_{s,i}$ is the average SU density on channel i.

The average fraction of areas where the channel is available at any given time can be approximated as:

$$\gamma_i \approx (1 - \chi_i) + \chi_i\, \varpi_{idle,i} = 1 - \chi_i\, \varpi_{busy,i}, \tag{6}$$

where $\varpi_{idle,i} = 1 - \varpi_{busy,i}$ is the steady-state probability that a PU on channel i is in `idle` state, i.e., not transmitting data.

B. Assumptions for Modeling Channel Availability

To model channel availability from a mobile SU perspective, we make the following three main assumptions:

- **A1)** PUs' traffic statistics, i.e., `busy`/`idle` periods follow exponential distributions.
- **A2)** The time interval that an SU moves inside a PPR follows exponential distributions.
- **A3)** The time during which an SU is located within a PPR follows exponential distributions.

Regarding **A1)**, the exponential distribution is the most widely used for modeling PU traffic patterns in CRNs. A recent measurement study [16] indicates that the PU channel-usage pattern can indeed be accurately approximated as an exponential distribution unless the average `busy`/`idle` periods are very long.[3]

[3]For such channels with long `busy`/`idle` periods, a long-tail distribution, such as log-normal distribution, is more suitable.

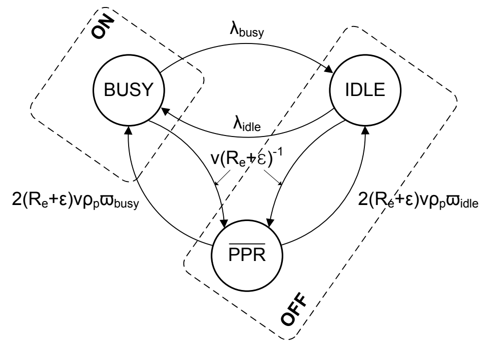

Fig. 4. **Mobility-aware channel availability model as a continuous-time Markov chain (CTMC):** A channel is available for a (mobile) SU either when (i) the SU located outside the PPRs (denoted as $\overline{\text{PPR}}$) or (ii) the primary transmitter of the PPR that the SU belongs to is in `idle` state.

Regarding **A2)**, let T_{hit} denote the first (hitting) time that a mobile SU n moves into an active PU's PPR (i.e., in `busy` state). Then, the analysis of T_{hit} is analogous to the hitting time of a stationary object in wireless sensor networks, which can be considered as a PU in a mobile CRN. By borrowing the analysis in [26], T_{hit} can be approximated as [26]:

$$T_{hit,n} \sim Exp(2(R_{e,i} + \epsilon_i)\bar{v}_n \rho_{p,i} \varpi_{busy,i}), \tag{7}$$

where $\bar{v}_n$ is the average speed of SU n.

Regarding **A3)**, the time duration in which an SU stays within a PPR can be derived from the link-lifetime distribution analysis in mobile ad-hoc networks [27]. According to [27], the link lifetime, i.e., the time duration during which the transmitter-receiver pair are located closer than a transmission range, can be accurately approximated as an exponential distribution with intensity, $\frac{\bar{v}}{R}$, where $\bar{v}$ is the average relative speed of the transceiver and R is the transmission range.

C. Mobility-Aware Channel Availability Model

We now opt to design a mobility-aware channel availability model for mobile CRNs. For this, we first define three states–i.e., `busy`, `idle`, and $\overline{\text{PPR}}$–based on the SU's location relative to the PPRs and PUs' traffic patterns, as shown in Fig. 4. We assume that channel i is available (i.e., OFF state) when a mobile SU is located outside the PPR of any *active* primary transmitters on channel i (i.e., `idle` or $\overline{\text{PPR}}$); otherwise, the channel is not available (i.e., ON state). We can thus reduce the Markov chain into a two-state model by merging the states `idle` and $\overline{\text{PPR}}$ into an OFF state, as shown in Fig. 4.

The ON/OFF state transitions occur in the following cases.

- **ON→OFF**: An SU moves out of the protection region of an active PU or a PU stops transmitting data.
- **OFF→ON**: An SU moves into the protection region of an active PU or a PU starts transmitting data.

We now derive the distributions of ON and OFF durations based on the Markov model in Fig. 4.

1) Distribution of "ON" Period: The sojourn time of the ON state of channel i follows an exponential distribution [27]:

$$T_{on,i} \sim Exp\Big(\lambda_{busy,i} + \frac{\bar{v}_n}{R_{e,i} + \epsilon_i}\Big), \tag{8}$$

where $\lambda_{busy,i}$ is the rate at which a PU resumes data transmission, $\bar{v}_n$ the average speed of an SU,[4] and $R_{e,i}$ and ϵ_i are the keep-out radius and the guard distance on channel i, respectively.

[4]Although the speed of an SU can vary depends on its movement pattern, we consider average speed in the analysis for mathematical tractability.

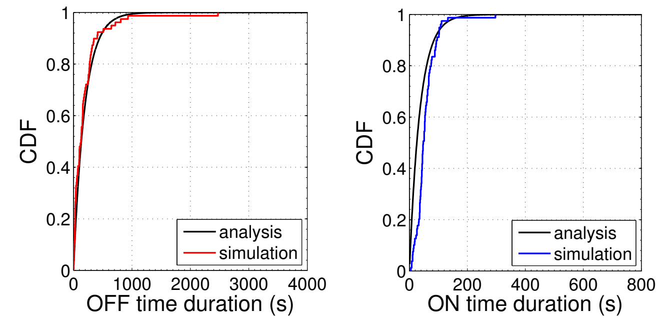

(a) OFF period (b) ON period

Fig. 5. **Comparison of channel ON/OFF duration distributions**: Our analyses on channel ON/OFF durations closely match the simulation results, thus corroborating the validity of the proposed channel model. In the simulation, we use the Random Waypoint model with no pause time where an SU uniformly chooses its speed in $[1, 10]$ m/s and destination with a fixed interval of 60 seconds. The average PU and SU densities are set to 2 and 10 (per km^2), respectively. We set $\varpi_{idle,i} = 0.4$ and $\lambda_{idle,i} = 0.01\, \forall i \in \mathcal{K}$.

2) Distribution of "OFF" Period: The OFF period duration can be thought of as the hitting time of the `busy` state, having either `idle` or $\overline{\text{PPR}}$ as an initial state. The OFF→ON state transition rate, λ_{off}, can be derived using the detailed balance equation, i.e., $\varpi_{on,i}\lambda_{on,i} = \varpi_{off,i}\lambda_{off,i}$, based on the stationary distributions of ON/OFF states, which can be approximated from Eq. (6), i.e., $\varpi_{on,i} = 1 - \gamma_i$ and $\varpi_{off,i} = \gamma_i$, and the ON→OFF transition rate $\lambda_{on,i}$ in Eq. (8), i.e.,

$$\lambda_{off,i} = \frac{\chi_i \varpi_{busy,i}}{1 - \chi_i \varpi_{busy,i}} \Big(\lambda_{busy,i} + \frac{\bar{v}_n}{R_{e,i} + \epsilon_i}\Big), \tag{9}$$

and thus, the sojourn time of the OFF state is given as:

$$T_{off,i} \sim Exp(\lambda_{off,i}). \tag{10}$$

The above analysis for channel modeling will be used for designing efficient spectrum sensing scheduling and distributed access strategy in Sections V and VI.

3) Model Verification: To show the accuracy of the proposed channel-availability model, we measure the channel ON/OFF periods observed from a mobile SU via simulation for 2×10^4 seconds. Fig. 5 shows that the empirical results closely match the analytical results, indicating the accuracy of the proposed model. To further quantify the accuracy, we measure the similarity between the empirical c.d.f. and the analytical c.d.f. using *Kullback-Leibler Divergence* (KLD) [28]. The KLD for two exponential distributions with intensities μ_o and μ_1 can be calculated as:

$$\mathcal{D}_{KL}(\mu_o \| \mu_1) = \log(\mu_o) - \log(\mu_1) + \frac{\mu_1}{\mu_o} - 1. \tag{11}$$

Table I summarizes the average and standard deviation of KLD for the ON/OFF durations while varying the maximum speed of SUs in the range of $[2, 10]$ m/s. It shows that the KLD remains low for all simulated scenarios. In fact, the case where $v_{max} = 10$ m/s corresponds to the case in Fig. 5.

V. Primary Protection via Joint Optimization of Spectrum Sensing Interval and Guard Distance

In this section, we jointly design the sensing interval and guard distance to protect PU communications from mobile SUs. We first derive the minimum spectrum sensing interval

TABLE I
KULLBACK-LEIBLER DIVERGENCE FOR CHANNEL MODEL

v_{max} (m/s)	$\mathcal{D}_{KL,OFF}$		$\mathcal{D}_{KL,ON}$	
	mean	std	mean	std
2	0.0441	0.0513	0.0069	0.0028
4	0.0413	0.0456	0.0202	0.0269
6	0.0301	0.0410	0.0848	0.0511
8	0.0875	0.0485	0.0982	0.0415
10	0.2335	0.0942	0.3134	0.1605

for mobile SUs, and then the optimal guard distance that maximizes spatio-temporal spectrum opportunities.

A. Mobility-Aware Spectrum Sensing

In order to avoid causing excessive interference to primary communications, SUs must perform spectrum sensing frequently enough to detect a primary signal before they move into the PPR of active PUs. We assume that SUs can perfectly detect the presence of a primary signal via spectrum sensing when they are located within the PPR of any active PU. In practice, SUs may need to adjust the sensing parameters to identify their locations relative to the PPRs, but this is not within the scope of this paper.

There are two conditions under which an SU performs spectrum sensing: (i) when the c.d.f. of the channel OFF state at a given time exceeds a predefined threshold, ξ $(0<\xi<1)$, to detect the returning PUs, or (ii) when an SU travels a certain distance since the previous sensing time, to prevent an SU from moving into the keep-out radius, whichever comes first.

Then, the minimum sensing interval required on channel i is given as:

$$t_i^* = \max\left\{T_{s,i}, \min\left\{-\frac{\ln(1-\xi)}{\lambda_{off}}, \frac{\epsilon_i}{\bar{v}}\right\}\right\}, \qquad (12)$$

where λ_{off} is the intensity of the channel OFF period distribution in Eq. (9), ϵ_i the guard distance, and $\bar{v}$ the average speed of an SU. Note that a lower probability ξ will lead SUs to sense the channel more frequently.

Eq. (12) indicates that the minimum sensing interval depends not only on *temporal* features such as primary traffic statistics, but also on *spatial* features such as the SUs' average speed $\bar{v}_n$ and the PU density $\rho_{p,i}$.

Fig. 6(a) shows that when an SU moves slowly (Region **I** for the case $\epsilon=40$ m), the sensing interval will be determined by PU traffic patterns, i.e., λ_{busy} and λ_{idle}, whereas, when it moves quickly (Region **II**), the interval will be determined by the speed of SUs. We have made a similar observation regarding PU density in Fig. 6(b).

B. Design of Optimal Guard Distance

The selection of guard distance, ϵ, entails an interesting tradeoff in exploring the spectrum opportunities in the time and space domains. That is, a larger guard distance (thus enlarging the areas of PPRs) will reduce the spatial spectrum opportunities. However, this allows SUs to perform sensing less frequently and spend more time for data transmission, thus increasing the spectrum opportunities in the temporal domain.

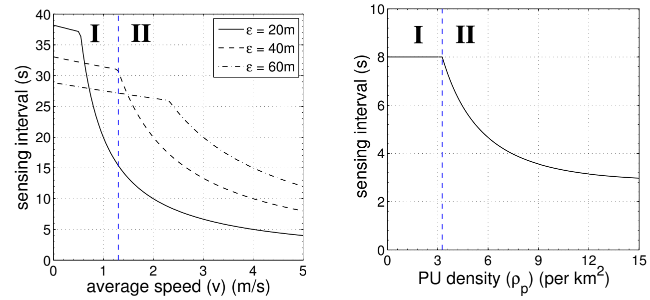

(a) Impact of SU mobility (b) Impact of PU density

Fig. 6. **Minimum sensing interval:** Sensing interval depends on (a) the SUs' average speed, $\bar{v}$, and (b) the average PU density, ρ_p. In our simulation, we set the parameters $\xi=0.3$, $\epsilon=40$ m, $\rho_s=10/\text{km}^2$, $\rho_p=1/\text{km}^2$, $R_o=250$ m, $\bar{v}=5$ m/s, $\lambda_{idle,i}=0.1$, and $\varpi_{idle,i}=0.4\,\forall i\in\mathcal{K}$.

Definition 3 *(Average channel utilization)* Average channel utilization *is defined as the average fraction of time a mobile SU can access the channel $i\in\mathcal{K}$, i.e.,*

$$u_{i,n} = \mathbb{E}\left\{1 - \frac{\sum_{j=1}^{N_{s,i,n}} T_{s,i} - T_{sw,i}}{T_i}\right\}, \qquad (13)$$

where $N_{s,i,n}$ is the number of times SU n performs spectrum sensing within the channel access epoch T_i. $T_{s,i}$ and $T_{sw,i}$ are the times spent for a one-time sensing and switching for channel i, respectively. Without loss of generality, we assume $T_s=T_{s,i}\ \forall i$ and $T_{sw}=T_{sw,i}\ \forall i$.

Definition 4 *(Spatio-temporal spectrum opportunity) The availability of channel $i\in\mathcal{K}$ in the spatio-temporal domain, denoted as Λ_i, is defined as the long-term average fraction of the time a mobile SU can access the channel, i.e., $\Lambda_i=\gamma_i u_i$ where γ_i and u_i are defined in Eqs.* (6) *and* (13)*, respectively.*

Fig. 7(a) plots the spatio-temporal channel availability Λ_i for various guard distances ϵ_i. As shown in the figure, when ϵ_i is too small (i.e., $\epsilon_i<3$ m), Λ_i is 0 because of the need to sense the channel continuously, i.e., $t_i^*=T_{s,i}$. When ϵ_i is relatively small, Λ_i suffers from a large (temporal) sensing overhead, whereas when ϵ_i is too large, Λ_i suffers from decreased spatial spectrum opportunities.

Proposition 1 *(Optimal guard distance) The optimal guard distance ϵ^* that maximizes spatio-temporal spectrum opportunity, Λ_i, is given as:*

$$\epsilon_i^* = \frac{R_{e,i}\bar{v}\,T_{s,i} + \sqrt{(R_{e,i}\bar{v}T_{s,i})^2 + \frac{2\bar{v}T_{s,i}(R_{e,i}-\bar{v}\,T_{s,i})}{\pi\rho_{p,i}\varpi_{busy,i}}}}{2(R_{e,i}-\bar{v}T_{s,i})}, \qquad (14)$$

where $R_{e,i}$ is the keep-out radius, $\bar{v}$ the average speed of SUs, $T_{s,i}$ the sensing time, $\rho_{p,i}$ the primary density, and $\varpi_{busy,i}$ the steady-state probability of a `busy` *state for channel i.*

Proof: The average fraction of area which is not covered by the PPRs can be approximated as $\gamma_i(\epsilon_i)\approx e^{-f(\epsilon_i)}$ from Eq. (6) where $f(\epsilon_i)=\rho_{p,i}\varpi_{busy,i}\pi(R_{e,i}+\epsilon_i)^2$. Assuming the switching overhead is negligible compared to the average OFF period, i.e., $T_{sw}\ll\lambda_{off}^{-1}$, u_i can be approximated as $u_i\approx 1-\frac{\bar{v}\,T_{s,i}}{\epsilon_i}$. Then, the channel availability in the spatio-temporal domain can be expressed as:

$$\Lambda_i(\epsilon_i)\approx\gamma_i(\epsilon_i)u_i(\epsilon_i)\approx e^{-f(\epsilon_i)}\Big(1-\frac{\bar{v}\,T_{s,i}}{\epsilon_i}\Big). \qquad (15)$$

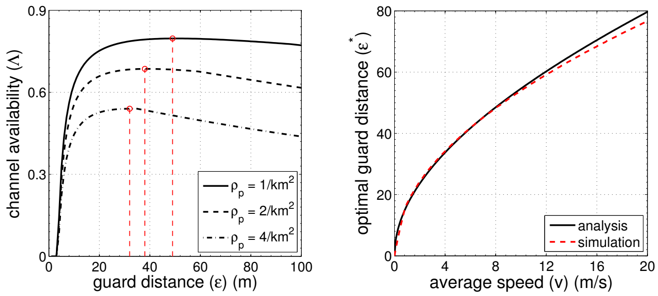

(a) Impact of guard distance (b) Optimal guard distance (ϵ^*)

Fig. 7. **Optimal guard distance** (ϵ^*): (a) The channel availability Λ_i depends significantly on the design of guard distance, and (b) the optimal guard distance differs for different SU mobilities. The parameters are set to $\rho_s = 10/\text{km}^2$, $\lambda_{idle,i} = 0.1$, $\varpi_{idle,i} = 0.4 \, \forall i \in \mathcal{K}$, and $\rho_p = 2/\text{km}^2$ in (b).

It can be easily shown that $\frac{\partial^2 \Lambda_i(\epsilon_i)}{\partial \epsilon_i^2} < 0$. By taking the first-order derivative of $\Lambda(\epsilon_i)$ and setting it to zero, we have:

$$\frac{\partial \Lambda_i(\epsilon_i)}{\partial \epsilon_i} = e^{-f(\epsilon_i)}\left(-2\rho_{p,i}\varpi_{busy,i}\pi(R_{e,i}+\epsilon_i)\left(1-\frac{\bar{v}\,T_{s,i}}{\epsilon_i}\right) + \frac{\bar{v}\,T_{s,i}}{\epsilon_i^2}\right) = 0. \quad (16)$$

For mathematical simplicity, we assume that the term $2\rho_{p,i}\varpi_{busy,i}\pi\epsilon_i$ can be approximates as 0 in Eq. (16), which provides the following quadratic equation:

$$(R_{e,i} - \bar{v}\,T_{s,i})\epsilon_i^2 - R_{e,i}T_{s,i}\epsilon_i - \frac{\bar{v}\,T_{s,i}}{2\pi\rho_{p,i}\varpi_{busy,i}} = 0. \quad (17)$$

Then, by solving Eq. (17), the proposition follows. ■

Interestingly, Fig. 7(b) shows that, the optimal guard distance increases as SUs' average speed increases, which result from balancing the tradeoff between temporal and spatial spectrum opportunities—i.e., it is better to increase the guard distance at the cost of reduced spatial spectrum opportunity, rather than reducing the sensing interval. The figure shows that our analytical results closely match the exhaustive-search-based simulation results.

VI. Distributed Spectrum Access Strategy in Mobile CRNs

We now derive an optimal channel selection (access) strategy that maximizes each secondary link's throughput. In multi-user CRNs, it is important to consider the channel contention overhead, as it can affect the achievable throughput significantly. However, it may be infeasible for mobile SUs to estimate the interference on each channel in real time. Thus, we assume that all the SUs in the network follow the same channel access strategy, and derive the optimal strategy by taking into account SUs' mobility-dependent spectrum opportunity as well as channel access contention among SUs as follows.

Let us denote the mixed channel selection vector by $\mathbf{p} = [p_1, p_2, \ldots, p_{|\mathcal{K}|}]^T$ where $\sum_{i\in\mathcal{K}} p_i = 1$. Then, the total number of SUs selecting channel i in the network can be approximated as Np_i, where N is the total number of SUs in the network, which can be estimated as $N \approx \rho_s A$. A is the entire network coverage area and ρ_s is the average SU density. The probability that an arbitrarily-chosen SU on channel i has $m \in \mathbb{N}$ interfering neighbors, that have chosen the same channel, follows a Binomial distribution, i.e., $M_i \sim B(m; Np_i - 1, f_i)$. Here, $f_i = \frac{\pi R_{I,i}^2}{A}$ is the ratio of the SU's interference region to the total network area, where $R_{I,i}$ is the interference range of an SU on channel i.

The expected throughput of secondary link n can then be expressed as:

$$E[R_n] = \sum_{i=1}^{K} p_i \sum_{m=0}^{Np_i-1} \frac{\Lambda_i}{m+1}\binom{Np_i-1}{m} f_i^m (1-f_i)^{Np_i-m-1} = \frac{1}{N}\sum_{i=1}^{K}\Lambda_i\left(\frac{1-(1-f_i)^{Np_i}}{f_i}\right), \quad (18)$$

where $K = |\mathcal{K}|$ is the total number of licensed channels.

Then, the problem of finding an optimal channel selection strategy $\mathbf{p}^\star$ can be cast into the following optimization problem (**P1**):

$$\text{minimize} \quad \mathbb{F}(\mathbf{p}) = -\sum_{i=1}^{K}\Lambda_i\left(\frac{1-\bar{f}_i^{Np_i}}{f_i}\right)$$

$$\text{subject to} \quad \sum_{i=1}^{K} p_i = 1 \quad \text{and} \quad \mathbf{p} \succeq 0,$$

where $\bar{f}_i = 1 - f_i$ for brevity.

To find the optimal sensing strategy $\mathbf{p}^\star$, we first show the convexity of $\mathbb{F}(\mathbf{p})$ by examining the second-order derivative of $\mathbb{F}(\mathbf{p})$ w.r.t. p_i, i.e.,

$$\frac{\partial^2 \mathbb{F}(p_i)}{\partial p_i^2} = \bar{f}_i^{Np_i}(\ln(\bar{f}_i^N))^2 > 0. \quad (19)$$

The inequality in Eq. (19) is straightforward. Hence, $\mathbb{F}(p)$ is convex in $\mathbf{p} \in [0,1]^K$.

Since the objective function is convex and constraints are affine, we now have a convex optimization problem. The Lagrangian with multipliers $\lambda \in \mathbb{R}^K$ and $\nu \in \mathbb{R}$ is given as:

$$L(\mathbf{p},\lambda,\nu) = \sum_{i=1}^{K}\Lambda_i(\bar{f}_i^{Np_i}\ln(\bar{f}_i^N))) - \sum_{i=1}^{K}\lambda_i p_i + \nu(\sum_{i=1}^{K} p_i - 1) = -\sum_{i=1}^{K}((\lambda_i - \nu)p_i - \Lambda_i(\bar{f}_i^{Np_i}\ln(\bar{f}_i^N)) - \nu,$$

where $\lambda \succeq 0$ and $\nu = 0$.

Then, the Lagrange dual function, i.e., the minimum value of the Lagrangian over $\mathbf{p}$, is given as:

$$g(\lambda,\nu) = \inf_{\mathbf{p}} L(\mathbf{p},\lambda,\nu) = \sum_{i=1}^{K}\inf_{\mathbf{p}}(-(\lambda_i-\nu)p_i + \Lambda_i(\bar{f}_i^{Np_i}\ln(\bar{f}_i^N))) - \nu.$$

It can be easily shown that there exists $\mathbf{p}$ such that the constraints hold with strict inequality, i.e., $p_i > 0 \, \forall i \in \mathcal{K}$ and $\sum_{i=1}^{K} p_i = 1$. Therefore, according to Slater's condition, strong duality holds with zero optimal duality gap.

The Karush-Kuhn-Tucker (KKT) conditions are given as:

$$\mathbf{p}^\star \succeq 0, \quad \sum_{i=1}^{K} p_i^\star = 1 \quad (20)$$

$$p_i^\star\left(\lambda^\star + \Lambda_i f_i^{-1}\bar{f}_i^{Np_i}\ln(\bar{f}_i^N)\right) = 0 \quad (21)$$

$$\lambda^\star + f_i^{-1}\bar{f}_i^{Np_i}\ln(\bar{f}_i^N) \geq 0. \quad (22)$$

Algorithm 1 OPTIMAL CHANNEL-SELECTION ALGORITHM

// **Initialization**
$\mathbf{p} \leftarrow [\frac{1}{K}, \ldots, \frac{1}{K}]^T$ // $\mathbf{p}$ is channel-selection probability
$\mathbf{p}_{prev} \leftarrow \mathbf{p}$
$\Delta \leftarrow \infty$
$\varepsilon \leftarrow 0.01$ // condition for the convergence
while ($\Delta > \varepsilon$) **do**
  Update the SU density on each channel $\rho_{s,i} \leftarrow \rho_s p_i$
  Update the keep-out radius $R_{e,i}$ using Eq. (3)
  Update the optimal guard distance ϵ_i^* using Eq. (14)
  Update the spatio-temporal channel availability $\Lambda_i(\epsilon_i^*)$
  Update the channel-selection vector $\mathbf{p}$ using Eq. (23)
  $\Delta \leftarrow \mathbf{p} - \mathbf{p}_{prev}$
  $\mathbf{p}_{prev} \leftarrow \mathbf{p}$
end while
return $\mathbf{p}$

By solving the above system of equations, we can derive the optimal channel-selection strategy, $\mathbf{p}^\star$, as described in the following proposition.

Proposition 2 *(Optimal channel-selection strategy) The optimal channel-selection vector $\mathbf{p}^\star$ that maximizes the expected secondary network throughput is:*

$$p_i^\star = \begin{cases} \left[\frac{-\ln(\Lambda_i)+\ln(f_i)+\ln(-N\ln(\bar{f}_i))-\ln(\lambda^\star)}{N\ln(f_i)}\right]^+ & \text{if } \varpi_{idle,i} > 0 \\ 0 & \text{if } \varpi_{idle,i} = 0, \end{cases} \quad (23)$$

where $\Lambda_i = \gamma_i u_i \, \forall i \in \mathcal{K}$ and $\lambda^\star$ is a constant s.t. $\sum_{i=1}^{K} p_i = 1$.

Eq. (23) indicates that the channel-selection probability p_i increases as the channel availability Λ_i increases, thus confirming our intuition. Interestingly, the optimal channel-selection vector $\mathbf{p}^\star$ in Eq. (23) depends on SU density on each channel as the number of SUs affects the selection of guard distance (in Eq. (6)), influencing the amount of spatial spectrum opportunity. This coupling between channel-selection strategy and spatial channel availability requires an iterative algorithm to find the optimal strategy, as described in **Algorithm** 1.

Proposition 2, however, provides the following counter-intuitive observation:

Corollary 1 *The optimal channel-selection probability becomes more uniform as the number of SUs in the network increases, i.e., $\forall i \in \mathcal{K}$,*

$$p_i^\star \rightarrow \frac{1}{K} \quad \text{as} \quad N \rightarrow \infty, \quad (24)$$

where K is the number of licensed channels, and N is the total number of SUs in the network.

Corollary 1 indicates that the optimal channel-selection probability becomes almost independent of spatio-temporal spectrum opportunities as SU density approaches infinity. The is because, when there exists a large number of SUs, the benefit from heterogeneous spatio-temporal spectrum opportunities becomes negligible due to high level of interference among SUs.

VII. PERFORMANCE EVALUATION

We evaluate the performance of the proposed spectrum sensing and distributed channel-selection schemes. We first describe the simulation setup, channel-selection schemes for performance comparisons and performance metrics. Then, we present key evaluation results.

A. Simulation Setup

We consider a CRN in which mobile SUs coexist with PUs in a $5\,\text{km} \times 5\,\text{km}$ area. Throughout the simulation, we assume that there are 5 licensed channels,[5] and that the average channel `idle` probability is in the range of $[0.3, 0.7]$, unless specified otherwise. We also assume that λ_{idle} is 0.1 for all the channels and that average density of SUs ρ_s ranges in $[1, 10]/\text{km}^2$. We assume that the path-loss exponent α is 4, the SUs' transmit power P_o is $100\,\text{mW}$, the reference distance d_o is $1\,\text{m}$, the PUs' transmission range R_o is $250\,\text{m}$, the interference temperature limit (`ITL`) is $0.1\,\text{mW}$, and the sensing triggering threshold ξ is 0.3. We further assume that channel sensing and switching times are $T_s = 0.5\,\text{s}$ and $T_{sw} = 1\,\text{s}$, respectively.

To comparatively evaluate the efficacy of the proposed channel-selection scheme, we compare the following: (i) random channel selection (`RAND`), (ii) optimal channel selection strategy based only on PUs' temporal channel usage statistics (`OPT-T`), and (iii) optimal channel selection strategy based on PUs' spatio-temporal channel usage statistics (`OPT-ST`). In `RAND`, SUs randomly select a channel with an equal probability. In `OPT-T`, SUs use the channel-selection probability in Eq. (23) while setting $\gamma_i = \varpi_{idle,i} \, \forall i \in \mathcal{K}$ (thus eliminating the impact of heterogeneous PU density on channels). On the other hand, In `OPT-ST`, SUs fully exploits the spatio-temporal channel-usage characteristics of PUs.

To quantify the efficacy of the proposed algorithms, we use the following three main performance metrics:

- normalized secondary network throughput, i.e., $\frac{\sum_n R_n}{N}$,
- throughput fairness (Jain's index [29]), i.e., $\frac{(\sum_n R_n)^2}{N \sum_n R_n^2}$, and
- normalized energy consumption in spectrum sensing, i.e., the fraction of time a CR device spent on sensing during channel access,

where R_n is the throughput of secondary link n, and N is the total number of secondary links in the network.

B. Optimal Channel Selection

1) Impact of Temporal Channel Availability: We first study the impact of PUs' temporal channel-usage statistics on the optimal channel-selection strategy. For this, we fix the PU density at $\rho_{p,i} = 1/\text{km}^2 \, \forall i \in \mathcal{K}$ and set different channel `idle` probabilities, i.e., $\boldsymbol{\varpi}_{idle} = [0.3, 0.4, 0.5, 0.6, 0.7]$ (ϖ_{idle} increases with increasing channel index).

Fig. 8(a) shows SUs' preference to access channels with a higher average channel `idle` probability, i.e., $p_i > p_j$ when $\varpi_{idle,i} > \varpi_{idle,j}$. Interestingly, when SUs are densely populated, i.e., $\rho_s = 10/\text{km}^2$, the impact of PUs' temporal channel-usage statistics on the channel-selection strategy decreases. This is clearly shown in Fig. 8(b) where the largest difference in the channel-selection probability (i.e., $|\max(\mathbf{p}^\star) - \min(\mathbf{p}^\star)|$) decreases with the increasing SU density. Intuitively, as the number of SUs in the network increases, their channel access time decreases due to the need for sharing the channel. Thus, as the density tends to infinity, the achievable throughput of SUs becomes close to 0, regardless of the PUs' channel usage statistics.

[5] Although the number of available channels depends on the wireless environments, we observed similar results for different numbers of channels.

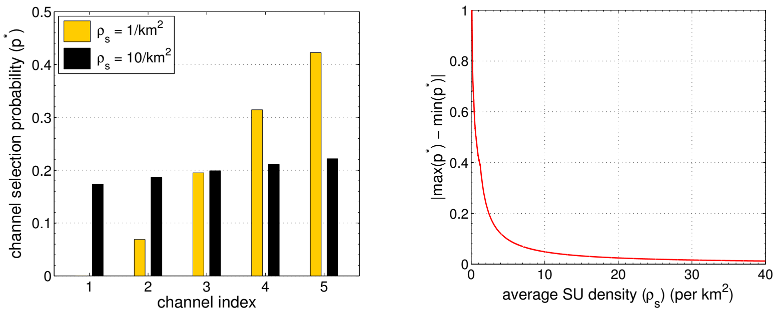

(a) Impact of channel availability

(b) Impact of SU density

Fig. 8. **Optimal channel-selection probability**: (a) The optimal channel-selection strategy depends on the average channel availability (ϖ_{idle}), but (b) the effects of PU traffic statistics decreases as SU density increases. The parameters are set to $\boldsymbol{\varpi}_{idle} = [0.3,\ 0.4,\ 0.5,\ 0.6,\ 0.7]$, $\bar{v}$ is fixed at $4\,\text{m/s}$, and $\rho_{p,i} = 1/\text{km}^2\ \forall i \in \mathcal{K}$.

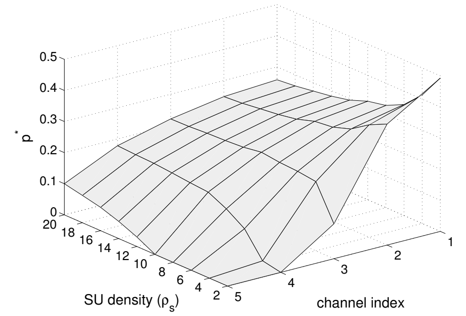

Fig. 9. **Impact of PU density on $\mathbf{p}^\star$**: Spatial distribution of PUs affects the optimal channel-selection probability. $\boldsymbol{\rho}_p = [0.1,\ 0.2,\ 0.5,\ 1,\ 2]/\text{km}^2$ (p_i increases with increasing channel index), $\varpi_{idle,i} = 0.4$ and $\lambda_{idle,i} = 0.1\ \forall i \in \mathcal{K}$.

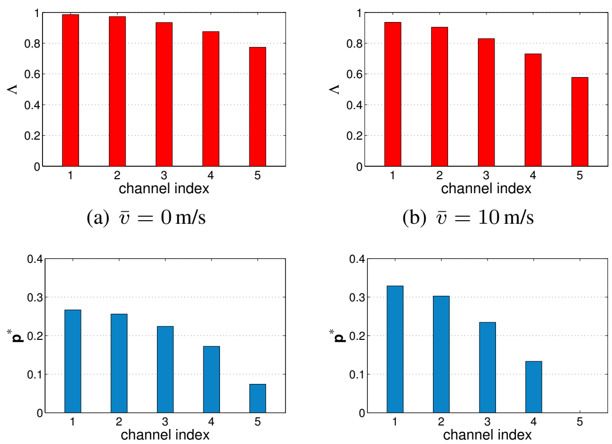

(a) $\bar{v} = 0\,\text{m/s}$

(b) $\bar{v} = 10\,\text{m/s}$

(c) $\bar{v} = 0\,\text{m/s}$

(d) $\bar{v} = 10\,\text{m/s}$

Fig. 10. **Impact of SUs' speed on Λ and $\mathbf{p}^\star$**: The spatio-temporal channel availability depends on the SUs' speed, thus affecting the optimal channel-selection strategy $\mathbf{p}^\star$. The parameters are set to $\boldsymbol{\rho}_p = [0.1,\ 0.2,\ 0.5,\ 1,\ 2]/\text{km}^2$, $\rho_s = 10/\text{km}^2$, and $\varpi_{idle,i} = 0.4\ \forall i \in \mathcal{K}$.

2) Impact of Spatial Channel Availability: Fig. 9 shows the impact of PU density on the optimal channel-selection strategy. In the simulation, we assume a different PU density on each channel, while assuming the temporal channel usage statistics, i.e., ϖ_{idle}, are the same for all channels. The figure indicates that, the lower the PU density (channel index), the higher the channel-selection probability. However, the PU density becomes less influential as the average SU density increases, similar to the case in Fig. 8(b).

3) Impact of SUs' Speed: Fig. 10 shows the impact of SUs' average speed on spatio-temporal channel availability Λ_i (in Figs. 10(a)-(b)), and on the optimal channel-selection strategy $\mathbf{p}^\star$ (Figs. 10 (c)-(d)). As shown in the figures, the SUs' speed has different consequences on channel availability (Λ), depending on the density of PUs on each channel; Λ decreases faster when PU density is high. As a result, the SUs' preference to access channels with a low PU density increases as their speed increases. The simulation settings are described in Fig. 10.

C. Performance Comparison

Next, we compare the performance of the three channel-selection schemes (i.e., `RAND`, `OPT-T`, and `OPT-ST`) in terms of throughput, fairness, and energy-efficiency. In the simulations, we set the average PU density on each channel to $\boldsymbol{\rho}_p = [0.1, 0.2, 0.5, 1, 2]/\text{km}^2$. The channel idle probabilities ϖ_{idle} are randomly selected in $[0,1]$ such that $\sum_{i\in\mathcal{K}} \varpi_{idle,i} = 1$ for each network topology. The results are obtained from simulation runs over 10^3 randomly-generated topologies. Figs. 11 and 12 plot the average and $\pm 0.25\,\sigma$ intervals of throughput and fairness, under various SUs' speed and density.

1) Throughput and Fairness: Fig. 11(a) shows that the proposed `OPT-ST` outperforms the other channel-selection schemes (i.e., `OPT-T` and `RAND`) under all simulated scenarios, thanks to its ability to optimally select channels by exploiting the heterogeneous spatial/temporal spectrum opportunities of each channel. On the other hand, the performance of `OPT-T` decreases as SU speed increases, because the spatial spectrum opportunity becomes more diverse with higher SU mobility (see Fig. 10), which is not considered in `OPT-T`. Fig. 11(b) indicates that `OPT-ST` achieves the highest fairness among the three channel-selection schemes, as it correctly incorporates the impacts of heterogeneous spectrum opportunities and channel access contention among SUs in the optimal channel selection strategy.

Fig. 12 shows the impact of SU density on throughput performance. As shown in the figure, the throughput degrades as SU density increases, mainly because of the increased level of SUs' contention for channel access. In addition, the performance of `OPT-ST` becomes close to `RAND`'s as the density increases, since the optimal channel-selection strategy tends to become similar to a uniform distribution, which can be seen in `RAND`, in a dense network, as observed in Fig. 9.

2) Energy Saving in Spectrum Sensing: Finally, we study the energy-saving perspective in spectrum sensing. Frequent spectrum sensing can consume a considerable amount of energy, especially in battery-powered mobile CR devices. Fig. 13 plots the CR's normalized energy consumption in different settings: use of a fixed guard distance (i.e., $\epsilon = 20, 40\,\text{m}$) and use of the optimal guard distance (ϵ^*). The figure indicates that energy consumption due to spectrum sensing in mobile CR devices can be reduced by up to $74\,\%$ while ensuring primary protection.

VIII. Conclusion

Taking mobility into consideration is vitally important for full realization of the benefits of opportunistic spectrum access

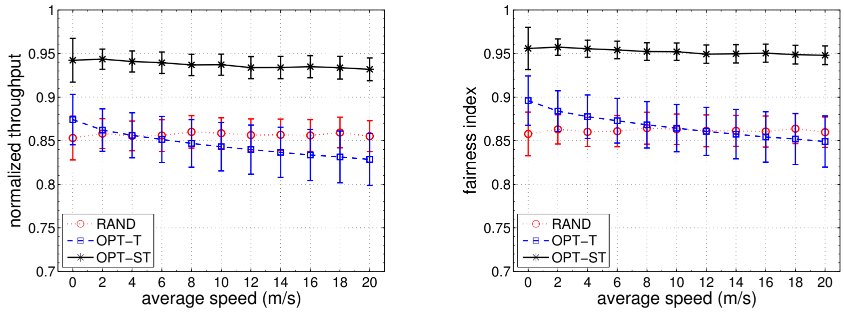

(a) Throughput (b) Fairness

Fig. 11. **Performance of the proposed distributed channel-selection algorithm**: OPT−ST outperforms other channel-selection schemes in terms of (a) network throughput and (b) fairness (Jain's index), under all simulated scenarios. In the simulation, the average SU density was fixed at $\rho_s = 1/\text{km}^2$.

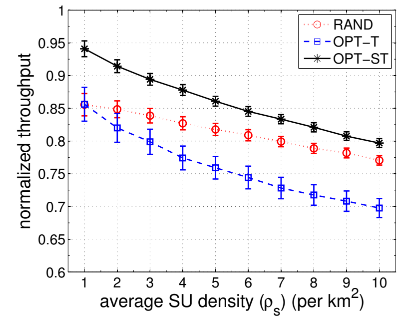

Fig. 12. **Impact of SU density on throughput performance**: The performance of OPT−ST decreases as the average SU density increases. In the simulation, the SUs' speed is fixed at 4 m/s.

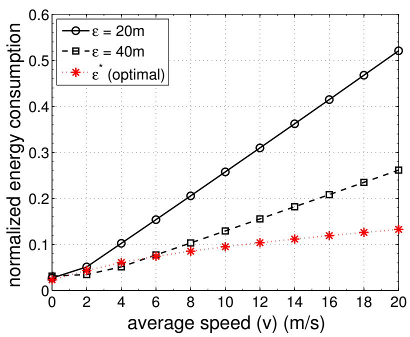

Fig. 13. **Energy savings via the use of optimal guard distance:** SUs can save energy significantly due to spectrum sensing via the optimal guard distance, while meeting the primary interference constraints.

in CRNs. In this paper, we considered the case of a CRN with mobile SUs. We identified and addressed the three fundamental challenges in maximizing spectrum efficiency in mobile CRNs. In particular, we presented a novel channel-availability model, a mobility-aware spectrum-sensing strategy, and an optimal distributed channel-selection (or access) strategy tailored to mobile CRNs. Our evaluation results verified the correctness of our channel-availability model under various SU mobility patterns. Our performance comparison study has also shown that the channel-access strategy improves the throughput and fairness of mobile SUs significantly over the conventional strategy that relies solely on PUs' temporal channel-usage statistics.

References

[1] Y.-C. Liang, Y. Zeng, E. C. Peh, and A. T. Hoang, "Sensing-Throughput Tradeoff for Cognitive Radio Networks," *IEEE Trans. Wireless Commun.*, vol. 7, no. 4, pp. 1326–1337, April 2008.

[2] A. W. Min and K. G. Shin, "An Optimal Sensing Framework Based on Spatial RSS-profile in Cognitive Radio Networks," in *Proc. IEEE SECON*, June 2009.

[3] A. W. Min, X. Zhang, and K. G. Shin, "Spatio-Temporal Fusion for Small-scale Primary Detection in Cognitive Radio Networks," in *Proc. IEEE INFOCOM*, March 2010.

[4] Q. Zhao, L. Tong, A. Swami, and Y. Chen, "Decentralized Cognitive MAC for Opportunistic Spectrum Access in Ad Hoc networks: A POMDP Framework," *IEEE J. Sel. Areas Commun.*, vol. 25, no. 3, pp. 589–600, April 2007.

[5] A. W. Min and K. G. Shin, "On Sensing-Access Tradeoff in Cognitive Radio Networks," in *Proc. IEEE DySPAN*, April 2010.

[6] A. W. Min, K. G. Shin, and X. Hu, "Attack-Tolerant Distributed Sensing for Dynamic Spectrum Access Networks," in *Proc. IEEE ICNP*, Oct 2009.

[7] IEEE 802.22 Working Group on Wireless Local Area Networks, http://www.ieee802.org/11/.

[8] J. Wang *et al.*, "First Cognitive Radio Networking Standard for Personal/Portable Devices in TV White Spaces," in *Proc. IEEE DySPAN*, April 2010.

[9] IEEE 802.22 Working Group on Wireless Regional Area Networks, http://www.ieee802.org/22/.

[10] A. T. Hoang, Y.-C. Liang, D. T. C. Wong, and R. Zhang, "Opportunistic Spectrum Access for Energy-constrained Cognitive Radios," *IEEE Trans. Wireless Commun.*, vol. 8, no. 3, pp. 1206–1211, March 2009.

[11] A. Dejonghe *et al.*, "Versatile Spectrum Sensing on Mobile Devices?" in *Proc. IEEE DySPAN*, April 2010.

[12] N. B. Chang and M. Liu, "Optimal Channel Probing and Transmission Scheduling in a Multichannel System," in *Proc. ACM MobiCom*, Sep 2007.

[13] A. T. Hoang and Y.-C. Liang, "Adaptive Scheduling of Spectrum Sensing Periods in Cognitive Radio Networks," in *IEEE Globecom*, Nov 2007.

[14] T. Shu and M. Krunz, "Throughput-efficient Sequential Channel Sensing and Probing in Cognitive Radio Networks Under Sensing Errors," in *Proc. ACM MobiCom*, Sep 2009.

[15] S. Huang, X. Liu, and Z. Ding, "Optimal Sensing-Transmission Structure for Dynamic Spectrum Access," in *Proc. IEEE INFOCOM*, April 2009.

[16] M. Wellens, J. Riihijärvi, and P. Mähöne, "Evaluation of Adaptive MAC-Layer Sensing in Realistic Spectrum Occupancy Scenarios," in *Proc. IEEE DySPAN*, April 2010.

[17] D. Cavalcanti and C. Cordeiro, "Proposed Resolution for Comments Related to the Superframe and Sensing," IEEE 802.22-07/0176r0, April 2007.

[18] FCC, "Second Report and Order," FCC 08-260, Nov 2008.

[19] M. Vu, N. Devroye, and V. Tarokh, "On the Primary Exclusive Region of Cognitive Networks," *IEEE Trans. Wireless Commun.*, vol. 8, no. 7, pp. 3380–3385, July 2009.

[20] M. F. Hanif, M. Shafi, P. J. Smith, and P. Dmochowski, "Interference and Deployment Issues for Cognitive Radio Systems in Shadowing Environments," in *Proc. IEEE ICC*, June 2009.

[21] Y. Yang, Y. Liu, Q. Zhang, and L. Ni, "Cooperative Boundary Detection for Spectrum Sensing Using Dedicated Wireless Sensor Networks," in *Proc. IEEE INFOCOM*, April 2010.

[22] D. Stoyan, W. S. Kendall, and J. Mecke, *Stochastic Geometry and its Applications*. Chichester: John Wiley & Sons, 1986.

[23] A. Fehske, J. Gaeddert, and J. H. Reed, "A New Approach to Signal Classification Using Spectral Correlation and Neural Networks," in *Proc. of IEEE DySPAN*, Nov 2005.

[24] R. Tandra and A. Sahai, "SNR Walls for Feature Detectors," in *Proc. IEEE DySPAN*, April 2007.

[25] J. Nieminen, R. Jäntti, and L. Qian, "Primary User Detection in Distributed Cognitive Radio Networks under Timing Inaccuracy," in *Proc. IEEE DySPAN*, April 2010.

[26] B. Liu, P. Brass, O. Dousse, P. Nain, and D. Towsley, "Mobility Improves Coverage of Sensor Networks," in *Proc. ACM MobiHoc*, May 2005.

[27] W. Wang and M. Zhao, "Joint Effects of Radio Channels and Node Mobility on Link Dynamics in Wireless Networks," in *Proc. IEEE INFOCOM*, April 2008.

[28] S. Kullback, *Information Theory and Statistics*. John Wiley and Sons, 1959.

[29] R. Jain, W. Hawe, and D. Chiu, "A Quantitative Measure of Fairness and Discrimination for Resource Allocation in Shared Computer Systems," Digital Equipment Corporation, Tech. Rep. DEC-TR-301, Sep 1984.